Biophysical Journal Volume 84 May 2003 3285–3298

Heme Structural Perturbation of PEG-Modified Horseradish Peroxidase C in Aromatic Organic Solvents Probed by Optical Absorption and Resonance Raman Dispersion Spectroscopy

Qing Huang,* Wasfi Al-Azzam,† Kai Griebenow,* and Reinhard Schweitzer-Stenner*

Departments of *Chemistry and †Biology, University of Puerto Rico, Río Piedras Campus, San Juan, Puerto Rico 00931-3346 USA

ABSTRACT The heme structure perturbation of poly(ethylene glycol)-modified horseradish peroxidase (HRP-PEG) dissolved in benzene and toluene has been probed by resonance Raman dispersion spectroscopy. Analysis of the depolarization ratio dispersion of several Raman bands revealed an increase of rhombic B_{1g} distortion with respect to native HRP in water. This finding strongly supports the notion that a solvent molecule has moved into the heme pocket where it stays in close proximity to one of the heme's pyrrole rings. The interactions between the solvent molecule, the heme, and the heme cavity slightly stabilize the hexacoordinate high spin state without eliminating the pentacoordinate quantum mixed spin state that is dominant in the resting enzyme. On the contrary, the model substrate benzohydroxamic acid strongly favors the hexacoordinate quantum mixed spin state and induces a B_{2g}-type distortion owing to its position close to one of the heme methine bridges. These results strongly suggest that substrate binding must have an influence on the heme geometry of HRP and that the heme structure of the enzyme-substrate complex (as opposed to the resting state) must be the key to understanding the chemical reactivity of HRP.

INTRODUCTION

Studying enzymes in nonaqueous solvents has emerged as a vivid and developing research area in biochemistry and biotechnology. This stems from the fact that many enzymes show new properties in organic solvents, i.e., the capability to catalyze reactions that do not take place in water (Klibanov, 1997) and solvent control of the stereoselectivity (Klibanov, 1990; Faber et al., 1993; Schoffers et al., 1996). However, enzymes are typically far less active in nonaqueous solvents than in the aqueous environment (Klibanov, 1997). This has resulted in enzyme activation in organic solvents being attempted by many groups using various strategies (see Griebenow et al., 1999, and references therein). One main difficulty in assessing the reasons for the changed enzyme activity in organic versus aqueous environment is that many factors influence enzyme activity in organic solvents, e.g., enzyme structure, conformational mobility, substrate and product solubility, and transition state solvation (Schmitke et al., 1996; Klibanov, 1997; Griebenow et al., 2001). In most applications, enzymes are used as dispersed dehydrated powders in organic solvents and more than crude secondary structure data have not yet become available to be related to the activity (Griebenow and Klibanov, 1997). Various methods used to solubilize enzymes in organic solvents (Paradkar and Dordick, 1994; Mabrouk, 1997) have become relevant in this context because they allow an assessment of the relationship between secondary and tertiary structure and enzymatic activity in these solvents (cf. e.g., Secundo et al., 1999). Generally, the fine structure of the respective active site cannot be explored under these conditions. Horseradish peroxidase (HRP), however, is an exception from this rule, because its active site is constituted by a chromogenic prosthetic heme group that can be selectively probed by resonance Raman spectroscopy. HRP has been widely employed as model enzyme in nonaqueous enzymology (see e.g., Kazandjian et al., 1986; Dordick et al., 1986; Gorman and Dordick, 1992; Ryu and Dordick, 1992) and it is involved in a variety of chemical reactions (Adam et al., 1999). Upon modification with poly(ethylene glycol) (HRP-PEG) and subsequent dissolution in benzene and toluene, the enzyme adopts a structure very similar to that in aqueous solution (Mabrouk, 1995; Mabrouk and Spiro, 1998; Al-Azzam et al., 2002).

HRP is a model system for exploring the enzymatic mechanisms of class III peroxidases and the underlying structure-function relationships due to its availability, remarkable catalytic activity, and stability in its natural aqueous environment as well as in a variety of organic solvents (Dunford, 1999; Kazandjian et al., 1986; Gorman and Dordick, 1992). The crystallographic structure of the wild-type of the most abundant isoenzyme HRPc and its complex with the model substrate benzohydroxamic acid (BHA) is well known (Fig. 1) (Gajhede et al., 1997; Henriksen et al., 1998). Covalent HRP modification with poly(ethylene glycol) greatly increases the solubility and reactivity in both hydrophilic and hydrophobic organic solvents, yielding homogeneous, optically transparent solutions (Takahashi et al., 1984; Mabrouk, 1995; 1997). HRP-PEG and its enzymatic intermediates in organic solvents have much better photostability and thermostability than in

Submitted September 6, 2002, and accepted for publication January 3, 2003.

Address reprint requests to Reinhard Schweitzer-Stenner, Dept. of Chemistry, University of Puerto Rico, Río Piedras Campus, PO Box 23346, San Juan, PR 00931-3346 USA. Tel.: 787-764-2417; Fax: 787-756-8242; E-mail: rstenner_upr_chemistry@gmx.net.

0006-3495/03/05/3285/14 $2.00

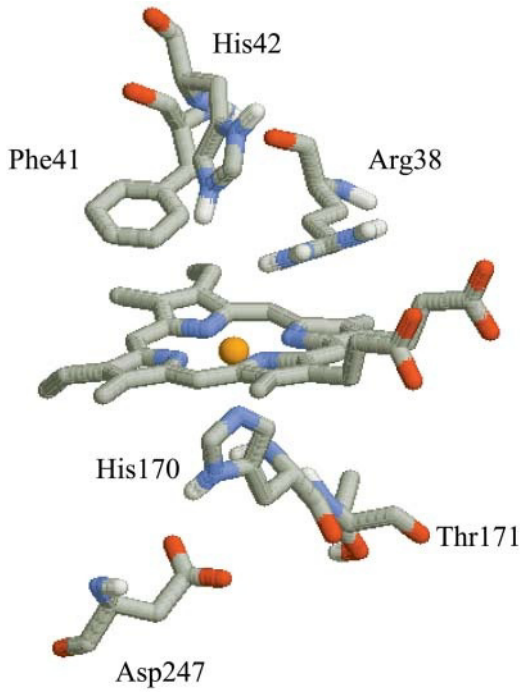

FIGURE 1 Crystallographic structure of HRP heme environment (Gajhede et al., 1997, Henriksen et al., 1998). Downloaded from the Protein Data Bank (1ATJ).

aqueous solution (Mabrouk, 1995) so that they become amenable to spectroscopic studies.

It has been shown that enzymatic activity and structural integrity of lyophilized HRP is retained in various organic solvents, especially in benzene and toluene (Kazandjian et al., 1986). The structure of dehydrated HRP-PEG dissolved in organic solvents essentially resembles the structure of native HRP in water (Ryu and Dordick, 1992; Kamiya et al., 2000; Al-Azzam et al., 2002). Despite the striking similarities in structure and enzymatic activity, however, special properties have been reported for HRP in some aromatic organic media, such as BHA (Teraoka and Kitagawa, 1981) and benzene (Mabrouk and Spiro, 1998). Akasaka et al. (1995) showed that HRP efficiently catalyzes the hydroxylation of benzene in the presence of H_2O_2, similar to what was obtained for cytochrome P450. Since the redox potential of benzene is higher than that of HRP in all its intermediates, an electron transfer can be ruled out as causing this reaction. Akasaka et al. found that 95% of the oxygen incorporated into the phenol product was from peroxide, a finding consistent with an oxo transfer mechanism. From their resonance Raman data, Mabrouk and Spiro (1998) proposed that such a mechanism requires the benzene molecule to slip into the heme pocket where it has to be located adjacent to the ferryl oxygen of compound I and thus also in close proximity to the heme group. They further hypothesized that this process is facilitated by the following structural alterations in the heme pocket: 1), A benzene molecule is bound at Phe^{179}, which perturbs Gln^{176} and disrupts its H-bond to the heme propionate substituent. 2), A salt bridge is formed between one propionate and distal Arg^{38}. 3), The imidazole residue of His^{170} moves toward Asp^{247} more closely, thus weakening the Fe-N_ε(His^{170}) bond.

If this view of the HRP-benzene complex is correct, the interacting benzene molecule shall significantly perturb the symmetry of the heme macrocycle. Such a perturbation has already been identified for HRP-PEG:BHA complexes, which in the hexacoordinate ferrous state exhibit significant Q-band splitting at cryogenic temperatures (Kaposi et al., 2001). Since benzene is expected to be closer to the heme group, its symmetry-lowering deformation efficiency should be even stronger than that of BHA. Such deformations can be obtained by means of polarized resonance Raman dispersion spectroscopy (PRRDS) (Schweitzer-Stenner, 1989; Schweitzer-Stenner, 2001). This technique determines static normal coordinate deformations (SNCDs) introduced first by Schweitzer-Stenner et al. (1984) and later in greater detail by Shelnutt, Jentzen, and associates (Jentzen et al., 1998; Shelnutt, 2000). The concept roots from the fact that any distortion in the porphyrin macrocycle can be approximately described as the superposition of several basic deformations along the normal modes of the unperturbed macrocycle in its D_{4h} symmetry. For planar distortions of the heme macrocycle, the deformation types can be attributed to the symmetry representations A_{1g}, B_{1g}, A_{2g}, and B_{2g} of the D_{4h} point group (Shelnutt, 2000; Schweitzer-Stenner, 1989). PRRDS is an excellent probe of SNCDs. The technique involves the determination of the depolarization ratio dispersion (DPR) of intense and structure sensitive marker bands of the Raman spectrum. Whereas the DPR is independent of the excitation wavelength for the ideal D_{4h} symmetry, the SNCDs give rise to a mixing of different symmetries into the Raman tensor, which combined with interferences between different vibronic coupling mechanism causes the DPR to depend of the excitation wavelength (Schweitzer-Stenner, 2001).

In this study, we applied PRRDS to HRP-PEG dissolved in benzene and toluene and HRP-PEG:BHA in water. Polarized Raman spectra were measured with different excitation wavelengths covering the Q_v-band region of the optical spectrum. The data were analyzed by invoking basic group theoretical arguments to obtain changes of specific asymmetric heme distortions. We show that aromatic solvent molecules and BHA induce distortion of different symmetry types due to their different locations in the heme pocket. Particularly our data provide conclusive evidence that a benzene and a toluene molecule are located close to the heme group, in full support of the model suggested by Mabrouk and Spiro (1998). Our results led us to hypothesize that the symmetry-lowering distortion of the heme might decrease the dissociation barrier for the ferryl ligand in the compound I state to facilitate the hydroxylation of benzene.

Theoretical background of PRRDS

Details of the theory used to analyze the depolarization ratio dispersion and the resonance excitation profiles of porphyrin Raman lines have been published elsewhere (Schweitzer-Stenner, 2001). In this paper we confine ourselves to a brief, more qualitative discussion of the relationship between DPD and SNCD.

Porphyrins in D_{4h} symmetry

In the ideal case of identical C_m and C_β substituents, a porphyrin macrocycle exhibits a planar conformation of D_{4h} symmetry. In this case the two lowest excited states, Q and B, are twofold degenerate and exhibit E_u symmetry. As a consequence, only A_{1g}, B_{1g}, B_{2g}, and A_{2g} type modes are resonance Raman active with B- and Q-band excitation. Following McClain (1971), their respective tensors can be written as:

$$\alpha^{A_{1g}}=\begin{pmatrix} a_{1g}(\tilde{\nu}_L) & 0 \\ 0 & a_{1g}(\tilde{\nu}_L)\end{pmatrix} \quad \alpha^{B_{1g}}=\begin{pmatrix} b_{1g}(\tilde{\nu}_L) & 0 \\ 0 & -b_{1g}(\tilde{\nu}_L)\end{pmatrix}$$
$$\alpha^{A_{2g}}=\begin{pmatrix} 0 & a_{2g}(\tilde{\nu}_L) \\ -a_{2g}(\tilde{\nu}_L) & 0\end{pmatrix} \quad \alpha^{B_{2g}}=\begin{pmatrix} 0 & b_{2g}(\tilde{\nu}_L) \\ b_{2g}(\tilde{\nu}_L) & 0\end{pmatrix}. \tag{1}$$

Since no transitions polarized perpendicular to the molecular plane are of relevance for Raman scattering of in-plane modes for porphyrins in ideal D_{4h}, all z components of the Raman tensor $\hat{\alpha}$ are zero. The tensor elements are calculated as the coherent superposition of all scattering amplitudes brought about by Franck-Condon, Herzberg-Teller, and Jahn-Teller coupling within and between the above-mentioned excited states (Shelnutt et al., 1977; Zgierski and Pawlikowski, 1982; Schweitzer-Stenner, 2001). Though the tensor elements are functions of the excitation wave number $\tilde{\nu}_L$, the depolarization ratios of all Raman lines are frequency independent, namely $\rho = 0.125$ for A_{1g}, 0.75 for B_{1g} and B_{2g} modes, and ∞ for A_{2g} modes.

Asymmetric distortions of the porphyrin macrocycle

Peripheral substituents or interactions with a protein matrix give rise to symmetry-lowering distortions Δ of the porphyrin macrocycle, which can be described as a superposition of SNCDs $\delta\bar{Q}_i^{\Gamma_i}$ (Jentzen et al., 1998; Shelnutt, 2000):

$$\Delta=\sum_{\Gamma_i,i}\gamma_i^{\Gamma_i}\delta\bar{Q}_i^{\Gamma_i}, \tag{2}$$

where $\gamma_i^{\Gamma_i}$ denotes the amplitude of the distortion along the normal coordinate of the i-th vibration of D_{4h} symmetry Γ_i. As shown in recent analyses of isolated porphyrins and heme groups in various proteins, Δ is dominated by the normal coordinates of the lowest-frequency modes of the respective symmetry representations (Shelnutt, 2000).

To account for the above symmetry-lowering distortions, we expand the vibronic coupling operator of the mode $Q_r^{\tilde{\Gamma}_r'}$ ($\tilde{\Gamma}_r'$ is now the representation in the lower-symmetry group) into a Taylor series in first order:

$$\frac{\partial\hat{H}_{el}(q,Q)}{\partial Q_r^{\tilde{\Gamma}_r}}=\frac{\partial\hat{H}_{el0}(q,Q)}{\partial Q_r^{\Gamma_r}}+\sum_{\Gamma_a}\sum_i\frac{\partial^2\hat{H}_{el0}(q,Q)}{\partial Q_r^{\Gamma_r}\partial Q_i^{\Gamma_i}}\delta\bar{Q}_i^{\Gamma_i}. \tag{3}$$

To couple electronic states of E_u symmetry, the representation Γ_r' of the electronic operators in Eq. 3, i.e., the derivatives, must transform like A_{1g}, B_{1g}, B_{2g}, or A_{2g}. This requirement is met, if the product $\Gamma_i' = \Gamma_r \otimes \Gamma_i$ contains at least one of these four representations. Hence, the contribution Γ_r' in Eq. 3 to the vibronic coupling operator transforms like the representation Γ_r of the observed Raman mode multiplied with the representation Γ_i of the SNCDs. As an example, a distortion of $\Gamma_i = B_{2g}$ symmetry gives rise to a first order contribution by admixing a $\Gamma_r' = A_{2g}$ symmetry tensor into the Raman tensor of a mode exhibiting $\Gamma_r = B_{1g}$ symmetry in D_{4h}, so that the effective symmetry $\tilde{\Gamma}_r$ reads as $B_{1g} + A_{2g}$.

Thus, in the most general case of a sufficiently low symmetry, admixtures of A_{1g}, B_{1g}, B_{2g}, and A_{2g} tensors occur. As a consequence, the Raman tensor of the representation $\tilde{\Gamma}_r$ can be expressed as a linear combination of the D_{4h} tensors in Eq. 3, so that in the lower symmetry (Lemke et al., 1998):

$$\hat{\alpha}=\begin{bmatrix} a_{1g}(\tilde{\nu}_L)+b_{1g}(\tilde{\nu}_L) & b_{2g}(\tilde{\nu}_L)+a_{2g}(\tilde{\nu}_{Ll}) \\ b_{1g}(\tilde{\nu}_L)-a_{2g}(\tilde{\nu}_L) & a_{1g}(\tilde{\nu}_L)-b_{1g}(\tilde{\nu}_{Ll})\end{bmatrix}. \tag{4}$$

By using the invariants of the isotropic, anisotropic, and antisymmetric part of the Raman tensor, the DPR can be calculated to (Lemke et al., 1998):

$$\rho=\frac{3}{4}\cdot\frac{a_{1g}^2(\tilde{\nu}_L)+5a_{2g}^2(\tilde{\nu}_L)+2(b_{1g}^2(\tilde{\nu}_L)+b_{2g}^2(\tilde{\nu}_L))}{6a_{1g}^2(\tilde{\nu}_L)+2(b_{1g}^2(\tilde{\nu}_L)+b_{2g}^2(\tilde{\nu}_L))}. \tag{5}$$

Equation 5 shows that ρ becomes independent of $\tilde{\nu}_L$, if only one symmetry type is present and the Raman tensor is represented by one of the forms in Eq. 1. This is the case in D_{4h}, but also in D_{4d}, D_4, C_{4v}, and D_{2d}. As can be seen by group correlation tables, mixing of the D_{4h} representations A_{1g}, B_{1g}, B_{2g}, and A_{2g} occurs for all point groups with symmetries lower than these, e.g.: C_4, C_{2h}, D_2, C_{2v}. As a consequence, one obtains a dispersion of the DPR, because $a_{1g}^2(\tilde{\nu}_L), a_{2g}^2(\tilde{\nu}_L), b_{1g}^2(\tilde{\nu}_L)$, and $b_{2g}^2(\tilde{\nu}_L)$ depend differently on the excitation frequency (Schweitzer-Stenner, 2001).

MATERIALS AND METHODS

Chemicals

Horseradish peroxidase isoenzyme c (HRPc) was purchased from Biozyme Laboratories (San Diego, CA) as lyophilized powder with an activity of at least 250 U/mg (one U defined as the amount of enzyme that will catalyze the production of 1 mg of purpurogallin from pyrogallol in 20 s at 20°C and pH 6.0) and a Reinheitszahl >3; 1 M HCl, toluene, BHA, and sodium

bicarbonate buffer salts were purchased from Sigma-Aldrich (St. Louis, MO). M-PEG-succinimidyl propionate (mPEG) with a molecular weight of 5000 was purchased from Shearwater (Huntsville, AL), benzene was obtained from Fisher Scientific (Cagey, PR), and 2, 4, 6 trinitrobenzene-sulfonic acid (TNBSA) from Pierce (Rockford, IL).

Preparation of HRPc-PEG

HRPc was covalently modified with mPEG using a similar procedure as described (Al-Azzam et al., 2002). HRPc (50 mg) and mPEG (51.1 mg) were dissolved in 20 ml 0.1 M sodium borate buffer (pH 9.2) to achieve an approximate molar ratio of 1:3 (solvent-accessible lysine residues in HRPc-to-mPEG) and stirred for 3 h at 4°C. The reaction was quenched by the addition of 20 ml of 0.1 M potassium phosphate buffer (pH 7.0). Nonreacted mPEG, buffer salts, and nonmodified HRPc were removed by dialysis of the reaction mixture in bags with an exclusion cutoff of 50,000 from Spectrum Laboratories (Rancho Dominguez, CA) thrice against 1 L of nanopure water (>18 MΩ resistance) for 4 h. Subsequently, HRPc-PEG was lyophilized as described (Al-Azzam et al., 2002).

Determination of the extent of mPEG modification

An average of three mPEG-modified amino groups per HRP was obtained by means of the TNBSA method (Habeeb, 1966; Al-Azzam et al., 2002), which is comparable with the numbers obtained in earlier studies (Mabrouk, 1995; Al-Azzam et al., 2002).

Preparation of samples for resonance Raman measurements

Five samples were used in the measurements: a), native HRP in potassium phosphate buffer, pH 8.0, at a concentration 40 mg/ml; b), HRP-PEG in potassium phosphate buffer, pH 8.0, at a concentration 58 mg/ml; c), HRP-PEG in benzene at a concentration 55 mg/ml; d), HRP-PEG in toluene at a concentration 60 mg/ml; and e), HRP-PEG in Tris buffer, pH 8, at a concentration of 50 mg/ml with a BHA concentration of 5 mM.

UV-vis absorption spectroscopy

UV-visible (UV-vis) spectra were recorded at room temperature using a computerized spectrophotometer (Shimadzu 160) and quartz cells with 10 mm pathlength; ~0.1 mg/ml HRPc was dissolved in potassium phosphate buffer at pH 8. To obtain spectra in benzene and toluene, lyophilized HRP-PEG was dissolved in the solvents to achieve a concentration of 0.2 mg/ml. For HRPc-PEG:BHA the concentration was 0.5 mg/ml. The extinction coefficient of HRPc was determined to be 77.2 mM cm^{-1} at 403 nm by measuring the absorbance at 403 nm for HRPc at various concentrations up to 0.0136 mM with a computerized spectrophotometer (Shimadzu 160) and quartz cells of 10 mm pathlength. The HRPc protein concentration was determined using the bicinchoninic acid assay (Pierce) for the same concentration range. This experimentally determined extinction coefficient was used to obtain the accurate protein concentration for the various HRPc/HRPc-PEG samples. The concentration was employed to transform the experimentally obtained absorption into extinction coefficient spectra.

Raman spectroscopy

Raman spectra were measured at room temperature in backscattering geometry with a tunable Argon ion laser (Lexel 95). The laser system provides eight lines from 458 to 515 nm. Thus, it covers the Q-band excitation region. The laser beam passed through an interference filter for each excitation line and was focused onto a solution sample in a quartz cell. The applied laser power was typically 5–10 mW. The scattered light was dispersed by a triple-grating spectrometer (Jobin-Yvon, Edison, NJ) and the spectra were recorded by a liquid nitrogen cooled CCD camera (CCD3000 from Jobin-Yvon). Polarization analyzer and scrambler were inserted between collimator and entrance slit of the spectrometer to measure the two components polarized perpendicular (I_y) and parallel (I_x) to the polarization of the incident laser beam. The spectra were calibrated by means of the 1605 cm^{-1} band in benzene (Ferraro and Nakamoto, 1994) with an accuracy of 1 cm^{-1}. The heme Raman marker bands, i.e., ν_{21}, ν_4, ν_3, ν_{11}, ν_2, ν_{19}, and ν_{10} were clearly identified in the spectral region 1350–1700 cm^{-1} for HRP in aqueous solution. However, in benzene and toluene, some Raman marker bands overlap with solvent bands. For benzene, one observes two strong bands at 1605 and 1586 cm^{-1}; for toluene, three strong bands appear at 1604, 1585, and 1379 cm^{-1}. Using the spectra of pure solvents as reference, these solvent bands were subtracted from the spectra in the spectral treatment afterward.

Spectral analysis

All spectra were analyzed by the spectral fitting program MULTIFIT (Jentzen et al., 1996). The spectra were subjected to a global fit involving a consistent decomposition of Raman bands by using identical parameters such as halfwidth, frequency positions, and band profiles for both polarizations and all eight excitation wavelengths. The depolarization ratios ρ of the thus identified spectral lines were calculated as $\rho = I_y/I_x$. More details about this fitting procedure are described by Jentzen et al. (1996).

RESULTS AND DISCUSSION

Spectral analysis

Absorption spectra of ferric HRPc in water, HRPc-PEG in water, benzene, toluene, and HRPc-PEG:BHA in water were measured to investigate whether changes in the coordination, spin, and redox state of the heme iron occurred upon PEG-modification (Fig. 2 *A*) and dissolution in organic solvents or upon BHA binding (Fig. 2 *B*). To facilitate the comparison of these spectra, we have performed a heuristic spectral decomposition into five bands assignable to B_v, B_0 (Soret), Q_v, Q_0 and a porphyrin → iron charge transfer band. The results are listed in Table 1 in terms of peak position, spectral bandwidth, and integrated molar absorptivity. All spectral parameters of the respective bands of HRPc and HRPc-PEG are identical within the limit of accuracy (Table 1). Thus, PEG modification of HRPc did not cause any detectable changes in the absorption spectrum. Binding of BHA to HRPc-PEG significantly shifts the Soret absorption and the Q-band region to higher wavelengths, whereas the charge transfer band above 600 nm is shifted down. In addition, it significantly reduces the full width at half-maximum of the Soret band, as observed by Howes et al. (1997), and the oscillator strength of all bands in the spectrum. The corresponding spectral shifts of HRPc-PEG dissolved in toluene and benzene are even more pronounced (Fig. 2 *B*). Moreover, an increase of the Q_0-band's integrated absorptivity and halfwidth was observed, whereas the absorptivity of the B-bands and of the Q_v-band decreases concomitantly. These spectral changes were more pronounced than those

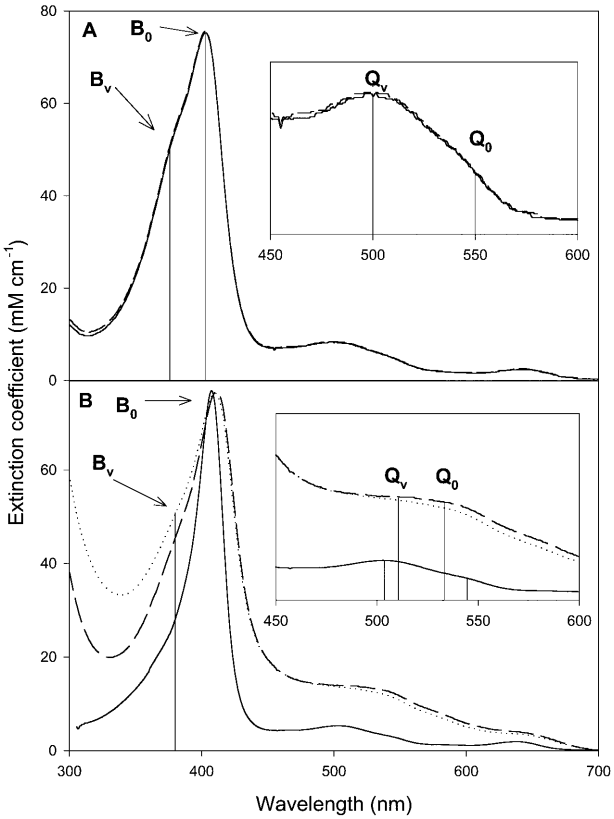

FIGURE 2 (*A*) UV-vis absorption spectra of HRPc (*full line*) and HRPc-PEG (*broken line*) in 10 mM phosphate buffer at pH 7. (*B*) UV-vis spectra of HRPc-PEG with 5 mM BHA in Tris buffer at pH 8 (*full line*), HRPc-PEG lyophilized from water pH 7 and redissolved in toluene (*short dashes*), and in benzene (*dotted line*). The insets show the region of Q absorption bands.

obtained in our previous investigation, for which a mixture of various HRP isoenzymes was employed (Al-Azzam et al., 2002). The spectral shifts are likely to result from electronic interactions between the respective solvent molecule and the E_g HOMOs of the macrocycle, which lower the energies of the latter and thus decrease the respective transition energy from the A_{2u} and A_{1u} LUMOs.

Fig. 3 depicts a set of Raman spectra recorded between 1300 and 1700 cm^{-1} for ferric HRP and HRP-PEG in different solvents with 457.9 nm excitation wavelength. The Raman spectrum of native HRP in aqueous solution is plotted in the bottom panel as a reference in which all characteristic heme bands, namely, ν_{21}, ν_4, ν_3, ν_{11}, ν_2, ν_{19}, and ν_{10} can be clearly identified, in accordance with the assignment by Smulevich and co-workers (Smulevich et al., 1994; Howes et al., 2001). The band profiles in Fig. 3 result from the spectral decomposition described in Materials and Methods. The spectral parameters of the most relevant bands are listed in Table 2. A significant overlap of ν_{10} with the bands of the C═C stretching modes of the two vinyl substituents at 1620 cm^{-1} and 1630 cm^{-1} (Smulevich et al., 1994) can be ruled out, because all three bands observed between 1615 and 1640 cm^{-1} are clearly depolarized (vide infra), whereas the localized and uncoupled vinyl modes (DeVito et al., 1992) give rise to polarized Raman bands. Unfortunately, an exact spectral analysis of the region between 1550 and 1600 cm^{-1} was rendered impossible due to the overlap of at least five different Raman bands. We heuristically decomposed this part of the spectrum into two representative bands at 1572 and 1583 cm^{-1} (Table 3). The effective wavenumbers of these two depend on the excitation wavelength since they result from overlapping contributions of ν_2/ν_{19a} and ν_2/ν_{19b}, respectively, where ν_{19a} and ν_{19b} represent conformers with different spin states of the heme iron (vide infra). All spectra were normalized onto the ν_4 band of HRP to compare the relative intensities of different Raman bands. HRP (Fig. 3, panel *A*) and HRP-PEG (panel *B*) in aqueous solution show no significant spectral differences between their respective wave numbers and intensities. This corroborates the notion that the tertiary structure of the heme cavity is maintained upon poly (ethylene glycol) modification (Mabrouk and Spiro, 1998; Al-Azzam et al., 2002). However, when HRP-PEG was dissolved in benzene (panel *C*) and toluene (panel *D*), some spectral discrepancies became apparent. The bandwidth of ν_4 is broadened by ~3 cm^{-1}. The relative intensities of ν_3 and ν_{11} are reduced in benzene and toluene. Since this broadening does not change the Lorentzian character of the band, it most likely results from a smaller dephasing time due to increased coupling with low frequency modes of the environment (Asher and Murtaugh, 1983; Schweitzer-Stenner et al., 1993). The band profiles of ν_{10} (Table 4) are similar in benzene and toluene, but slightly different from that of native HRP in aqueous solution. On the other hand, differences between the Raman

TABLE 1 Spectral parameters obtained from a five-band fit to the absorption spectra of HRPc and HRPc-PEG in water (with and without BHA) and organic solvents

HRP in water			HRP-PEG in water			HRP-PEG in benzene			HRP-PEG in toluene			HRP-PEG with BHA in water		
Peak [nm]	Width [nm]	A*	Peak [nm]	Width [nm]	A*	Peak [nm]	Width [nm]	A*	Peak [nm]	Width [nm]	A*	Peak [nm]	Width [nm]	A*
376 ± 1	39 ± 2	1417	376 ± 1	41 ± 2	1583	386 ± 2	43 ± 2	1025	384 ± 2	44 ± 2	1213	385 ± 1	41 ± 1	922
404 ± 1	29 ± 1	1723	404 ± 1	30 ± 1	1788	412 ± 1	29 ± 1	1377	412 ± 1	30 ± 1	1574	408 ± 1	21 ± 1	1361
504 ± 2	49 ± 1	153	503 ± 1	49 ± 1	175	523 ± 1	47 ± 3	69	523 ± 1	37 ± 3	61	507 ± 1	45 ± 1	108
537 ± 2	27 ± 2	27	536 ± 1	30 ± 2	35	546 ± 2	43 ± 3	46	548 ± 2	35 ± 3	54	542 ± 1	26 ± 1	15
645 ± 2	48 ± 3	138	647 ± 2	41 ± 3	122	650 ± 2	47 ± 2	84	650 ± 2	45 ± 2	77	639 ± 1	45 ± 1	130

*Integrated molar absorptivity (mM cm^{-1} nm).

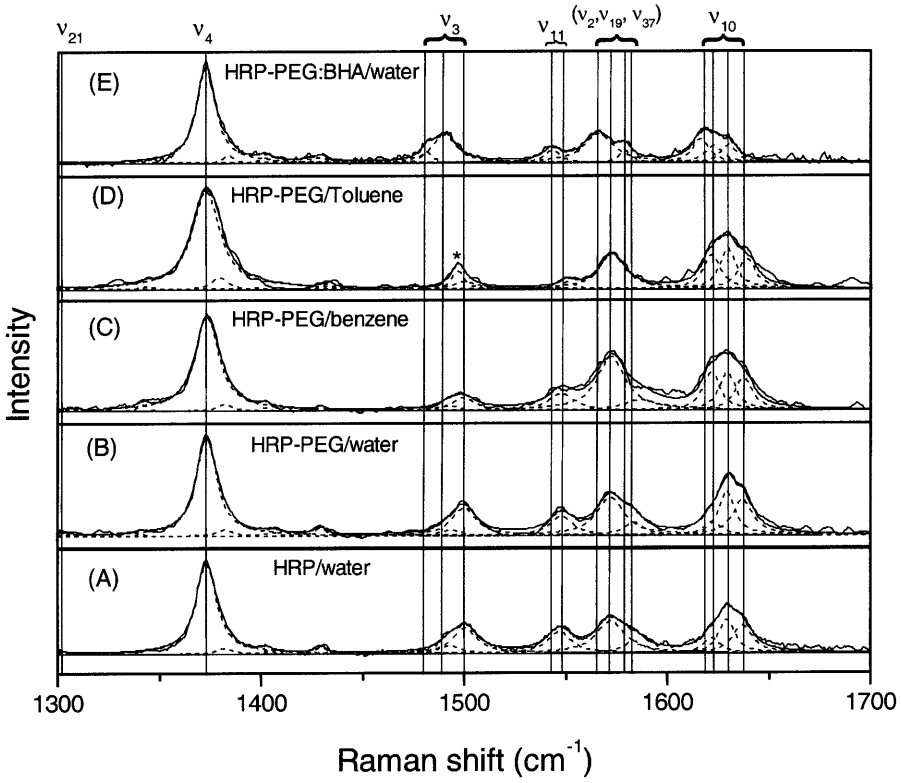

FIGURE 3 Raman spectra of ferric HRP under different experimental conditions with 457.9 nm excitation. (*A*) HRP in water, pH 8; (*B*) HRP-PEG in water, pH 8; (*C*) HRP-PEG in benzene; (*D*) HRP-PEG in toluene; (*E*) HRP-PEG:BHA in water, pH 8.

spectra of HRP-PEG in benzene and in toluene are negligible. Remarkable differences are observed, however, for HRP-PEG:BHA for which ν_3, ν_{11}, ν_2, and ν_{10} are all downshifted (panel *E*).

Spin and coordination state

To compare the iron spin and coordination states of the investigated samples, we first utilized the ν_3 band at around 1500 cm^{-1} because this band is well isolated and particularly spin sensitive (Spiro, 1985). In the spectra of native HRP, ν_3 contains at least two components at 1492 and 1500 cm^{-1}, which represent coexisting protein conformations with their iron atoms exhibiting pentacoordinate high spin (pc-hs) and pentacoordinate quantum mixed spin (pc-qms) states, respectively (Feis et al., 1998; Howes et al., 2000, 2001). The weaker band at 1492 cm^{-1} was previously assigned to a hexacoordinate high spin (hc-hs) (Rakshit and Spiro, 1974; Teraoka and Kitagawa, 1981; Evangelista-Kirkup et al., 1985; Palanappian and Terner, 1989.; Smulevich et al., 1991) and has recently been reassigned as pentacoordinated high spin state (Feis et al., 1998, Howes et al., 2000). We also assign it to pc-hs because this is consistent with the observation of a ν_{10} band at 1629 cm^{-1}, which is diagnostic of a pc-hs state for HRP (Smulevich et al., 1991, Feis et al., 1998, Howes et al., 2001) and also for barley (Howes et al., 1999) and soybean seed coat peroxidases (Nissum et al., 1998). These conformers are very likely to exhibit different distances between the proximal imidazole and the heme iron and, thus, different strengths of the axial ligand field. The 1500 cm^{-1} line of the pc-qms state is more intense than the 1492 cm^{-1} line of the pc-hs state in native HRP. Apparently, this is still the case for HRP-PEG in benzene even though the band profile appears somewhat more asymmetric toward the low wavenumber side indicating a somewhat higher occupation of the conformation with a pc-hs state. In toluene, the judgment of ν_3 signal is more difficult because this band is masked by a signal at 1497 cm^{-1}, which arises from neat toluene. Our results are somewhat at variance with the spectra of Mabrouk and Spiro, who found ν_3 to be downshifted from 1495 cm^{-1} to 1480 cm^{-1} in the spectrum of HRP-PEG in benzene. This would be indicative of a dominant hc-hs state. However, this discrepancy can be resolved by an analysis of the other spin marker lines. Although the existence of a conformer with a pc-qms state in HRP-PEG in benzene and toluene is verified by the observation of a ν_{11} band at 1547 cm^{-1}, its significantly reduced intensity is indicative of a much smaller fraction of the pc-qms conformer in benzene and toluene (Table 1). This notion is further corroborated by the intensity distribution of the three ν_{10} bands at 1621, 1629, and 1637 cm^{-1} in the spectra depicted in Fig. 3, which are assignable to conformers with hc-hs, pc-hs, and pc-qms states of the heme iron, respectively. For native HRPc, the fractional intensities with respect to the total intensity of all ν_{10} bands are 0.18 (hc-hs), 0.49 (pc-hs), and 0.33 (pc-qms) (Table 4), whereas the corresponding values for HRPc-PEG in benzene are 0.34, 0.38, and 0.28. For HRPc-PEG in toluene, similar values

TABLE 2 Spectral parameters of prominent marker bands in the resonance Raman spectra of native HRPc and HRPc-PEG in water and organic solvents taken with 457 nm excitation

	Wave number [cm^{-1}]	Bandwidth [cm^{-1}]	Fractional intensity	Assignment	Wave number [cm^{-1}]	Bandwidth [cm^{-1}]	Fractional intensity	Assignment
	HRP in water				HRP-PEG in water			
ν_4	1373	10.7	0.33		1373	10.7	0.32	
ν_3	1493	11.2	0.03	pc-hs*	1493	11.2	0.02	pc-hs*
	1500	13.0	0.10	pc-qms†	1500	13.0	0.10	pc-qms†
ν_{11}	1547	12.5	0.08	pc-qms†	1547	12.5	0.07	pc-qms†
ν_{10}	1622	8.5	0.05	hc-hs†	1622	8.5	0.04	hc-hs†
	1629	7.7	0.10	pc-hs†	1629	7.7	0.11	pc-hs†
	1637	10.2	0.09	pc-qms†	1637	10.2	0.11	pc-qms†
	HRP-PEG in benzene				HRP-PEG in toluene			
ν_4	1373	13	0.33		1373	15.6	0.45#	
ν_3	1492	11.2	0.01	pc-hs*	1493	11.2	0.005	pc-hs*
	1500	13.0	0.04	pc-qms†	1500	13.0	0.03	pc-qms†
ν_{11}	1547	13.4	0.06	pc-qms†	1547	10	0.04	pc-qms†
ν_{10}	1622	8.5	0.09	hc-hs†	1622	8.5	0.09	hc-hs†
	1629	7.7	0.08	pc-hs†	1629	7.7	0.10	pc-hs†
	1637	10.2	0.08	pc-qms†	1637	10.2	0.8	pc-qms†

The integrated intensities of the Raman lines are given as fraction of the total Raman scattering detected in the spectral region shown in Fig. 3.

Spectral parameters of prominent marker bands in the resonance Raman spectra of native HRPc and HRPc-PEG:BHA in water

	HRP				HRP-PEG with BHA			
ν_4	1373	13	0.33		1373	10	0.37	
ν_3	1492	11.2	0.01	pc-hs*	1490	12.3	0.13	hc-qms‡
	1500	13.0	0.04	pc-qms†				
ν_{11}	1547	13.4	0.06	pc-qms†	1543	7.8	0.04	hc-qms‡
ν_{10}	1622	8.5	0.09	hc-hs†	1617	8	0.08	hc-qms‡
	1629	7.7	0.08	pc-hs†	1622	8.2	0.05	vinyl§
	1637	10.2	0.08	pc-qms†	1630	7.3	0.05	vinyl§

*Interference from a toluene band at 1379 cm^{-1}.
†Howes et al. (2001).
‡Indiani et al. (2000).
§Smulevich et al. (1994).

were obtained (0.37, 0.38, and 0.25). This clearly shows that indeed the hc-hs conformer is somewhat stabilized in the employed aromatic solvents, although it still coexists with the two other spin and coordination states. (A direct determination of the molar fraction of the three conformers from the fractional intensities of the marker bands is not possible, because it is likely that the respective resonance excitation profiles are different in the preresonance and resonance region of the Q_v-band covered by the employed excitation wavelengths.) The difference between our ν_3 band profile and that reported by Mabrouk and Spiro (1998) can best be explained by the different excitation wavelengths employed. The 406-nm excitation used in their study can be assumed to predominantly enhance the hc-hs species because its absorption maximum is very likely close to this wavelength. This is in agreement with the Soret absorption maximum at 408 nm of HRPc-PEG in the presence of BHA (Fig. 2 *B*), where a hexacoordinated species is predominant (see below). The absorption maximum of the pc-qms state can be expected to be at a more blue-shifted position (Feis et al., 1998).

Different from HRP-PEG in neat organic solvents, HRP-PEG:BHA in aqueous solution seems to predominantly exist in a single conformation. Single ν_3 and ν_{10} bands were observed at 1491 cm^{-1} and 1618 cm^{-1}, respectively. The bands at 1622 and 1630 cm^{-1} are now attributed to vinyl vibration owing to its depolarization ratio. The marker bands ν_2 and ν_{11} are downshifted to 1568 and 1543 cm^{-1},

TABLE 3 Wave numbers (in units of cm^{-1}) obtained from the heuristic two-band fit to the region between 1550 and 1600 cm^{-1} and assignments to overlapping bands from ν_2, ν_{19}, and ν_{37}

		HRPc in water	HRP-PEG in water	HRP-PEG in benzene	HRP-PEG in benzene	HRP-PEG with BHA
$\nu_2 + \nu_{19} + \nu_{37}$	Peak 1	1572 ($\nu_2 + \nu_{19a}$)	1572 ($\nu_2 + \nu_{19a}$)	1572 ($\nu_2 + \nu_{19a}$)	1572 ($\nu_2 + \nu_{19a}$)	1567 (ν_2)
	Peak 2	1583 ($\nu_{19b} + \nu_{37}$)	1583 ($\nu_{19b} + \nu_{37}$)	1587 ($\nu_{19b} + \nu_{37}$)	–	1579 (ν_{19})

TABLE 4 Fractional intensities of ν_{10} (and vinyl) bands of HRPc and HRPc-PEG in water (with and without BHA) and organic solvents obtained from the decomposition of the 457 nm Raman spectrum between 1615 and 1640 cm^{-1}

	HRP	HRP-PEG	HRP-PEG in benzene	HRP-PEG in toluene	HRP-PEG with BHA
1617	–	–	–	–	0.43
1621	0.18	0.15	0.34	0.37	0.31 (vinyl)
1629	0.49	0.49	0.38	0.38	0.26 (vinyl)
1637	0.33	0.36	0.28	0.25	–

respectively (cf. Table 1). In earlier work, this observation has been interpreted as reflecting an hc-hs state (Smulevich et al., 1991, 1994; Teraoka and Kitagawa, 1981). This, however, is somewhat at odds with the crystal structure of HRPc:BHA (Henriksen et al., 1998), which exhibits a water-iron distance of 2.7 Å. If this is correct, the distal water would provide only a very weak axial field component, which should hardly affect the iron's electronic structure. Indeed, the value of 1491 cm^{-1} is somewhat too high for an hc-hs state. Based on EPR data, Indiani et al. (2000) have recently suggested that the iron-ligand complex in HRPc:BHA adopts an hc-qms rather than an hc-hs state.

Heme deformations

Fig. 4 illustrates the depolarization ratio dispersion (DPRD) for the ν_{21}, ν_4, and ν_{11} bands, which represent A_{1g}, A_{2g}, and B_{1g}like Raman modes, respectively. The depolarization ratios were determined from their integrated intensities as obtained from the spectra analysis. The reproducibility of the DPR-values for two different batches of HRP-PEG was found to be excellent. The DPRs of ν_4 in benzene and toluene are larger than the DPRs of native HRP in aqueous solution, whereas the DPRs of ν_{21} are smaller in nonaqueous solutions. Comparison of the DPRs of ν_{11}, however, show only modest differences between aqueous and nonaqueous solutions. In both cases, there the DPR increases with increasing excitation wavelength, but their deviation from 0.75 is not dramatic. The respective DPRs of HRP-PEG dissolved in benzene and toluene systematically exhibit lower values at nearly all excitation wavelengths. On the contrary, the DPRs of ν_{11} from HRP-PEG:BHA are much larger. This shows that the distortion symmetry types of the heme macrocycle are different for HRP in neat organic solvents and HRP-PEG:BHA in water.

The distortion types can be identified easily by analyzing the change of DPRs with wavelength in the framework of DPRD theory (Schweitzer-Stenner, 2001). We used this theory to simulate DPRs to qualitatively account for the dispersion curve for the ν_4, ν_{21}, and ν_{11} modes. For the sake of simplicity, we used only the first order term of the Raman tensor reported by Unger et al. (1993), thus neglecting multimode mixing. Since we consider asymmetrically distorted porphyrins, the Raman tensor was expressed as linear combination of McClain tensors for A_{1g}, B_{1g}, A_{2g}, and B_{2g} modes, as described above. A more detailed description and quantitative comparisons of simulations, which are of limited relevance in the context of this study, will be given elsewhere (Huang et al., 2003). The energies of the involved vibronic states, the transition dipole moments associated with the transitions into the Q- and B-states, and the respective Lorentzian bandwidths were estimated from the optical spectra. In Fig. 5, *a* and *b*, obviously, more B_{1g} and B_{2g} distortions can increase DPRs of A_{1g}like modes, but decrease DPRs of A_{2g}like modes effectively. The most likely patterns of these types of distortions are visualized in Fig. 6 (obtained from the home page of J.A. Shelnutt, http://jasheln.unm.edu). They depict the normal coordinates of the lowest frequency modes of B_{1g} and B_{2g} symmetry. B_{1g} is a rhombic deformation along the N-Fe-N line that involves displacement of the pyrrole nitrogen toward and away from the central iron atom along the respective symmetry axis. This distortion gives rise to the rhombicity of the ligand field of the central metal detected by EPR spectroscopy. B_{2g} involves a triclinic distortion along the C_α-Fe-C_α line and also significant asymmetric perturbation of the pyrrole rings. Although B_{1g} and B_{2g} distortions cannot be distinguished by the DPRs of *A*-type modes, they differently affect the DPRs of B_{1g}like modes. As illustrated by Fig. 5, *c* and *d*, an increase of B_{1g} distortions decreases the DPRs (Fig. 5 *c*); on the contrary, an increase of B_{2g} yields larger DPRs (Fig. 5 *d*). It follows from this simulation that an additional dominant B_{1g} in-planar distortion is imposed on the heme macrocycle of HRP-PEG in organic solvents.

This observation is consistent with the model suggested by Mabrouk and Spiro (1998) due to the following consideration. When HRP-PEG is dissolved in benzene and toluene, the aromatic molecules can slip into the active site due to their strong hydrophobic character. As a consequence, benzene or toluene behave like an aromatic substrate and perturb the H-bonding network. As postulated by Mabrouk (Mabrouk and Spiro, 1998), benzene becomes attached to Phe^{179}, thus positioning itself between Gln^{176} and one of the heme proprionic substituents. Thus, one can assume that the benzene interacts by $\pi\pi$-interactions with the pyrrole group to which the adjacent propionate is attached. This would make this particular pyrrole group inequivalent with the others. Group theoretically this can be described as a combination of B_{1g} and E_u distortions. The former is probed by our experiment. E_u distortions do not affect the DPRs shown in Fig. 4 but cause a Raman activity of E_u modes. It should be emphasized in this context that the proposed noncovalent coupling between the aromatic solvent molecule and the heme chromophore is also consistent with the

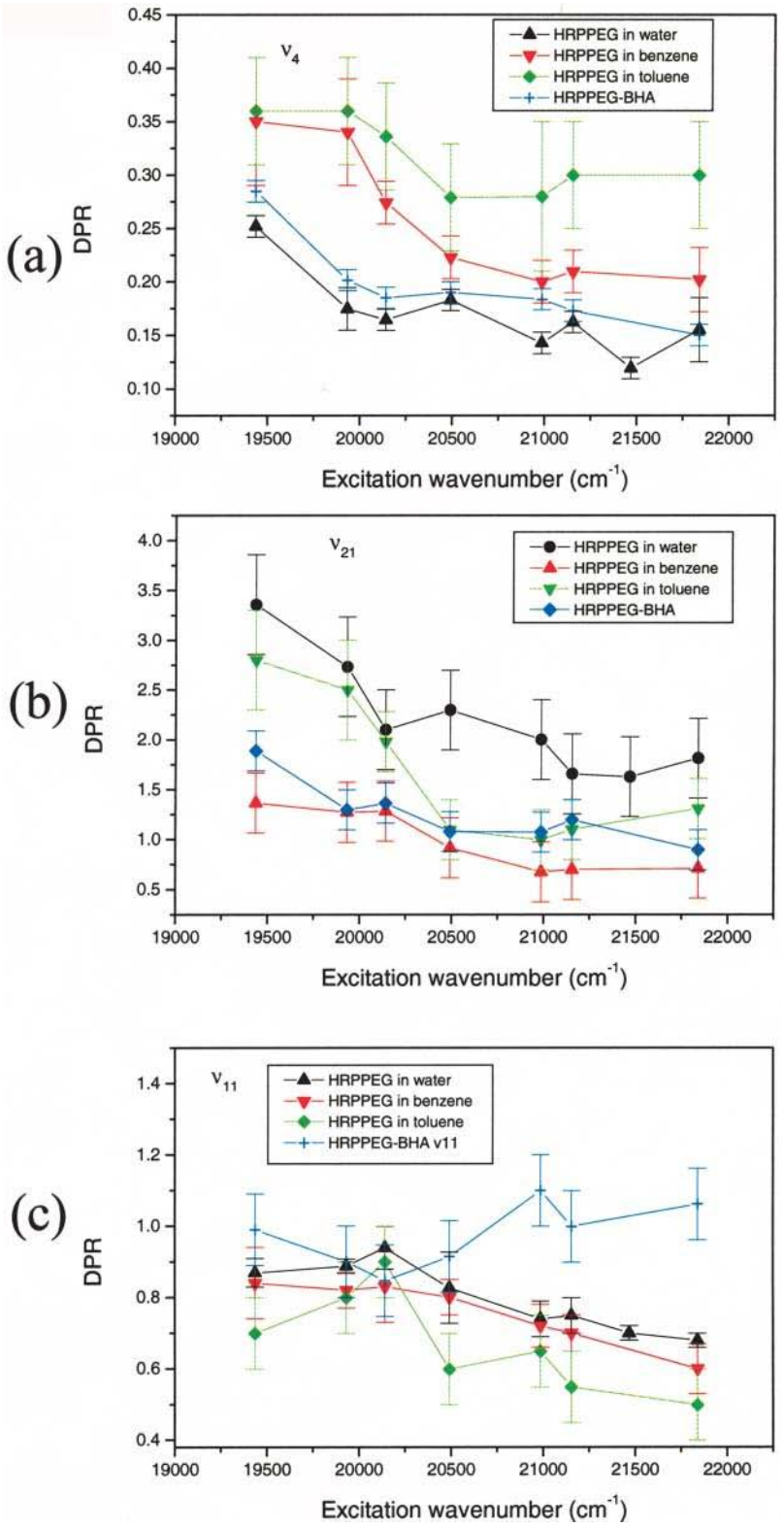

FIGURE 4 Comparison of the DPRs of (*a*) ν_4, (*b*) ν_{21}, and (*c*) ν_{11} mode for different HRP samples.

changes of above discussed changes of the optical absorption spectrum and requires that the solvent molecule is oriented parallel rather than perpendicular to the heme plane as suggested by Mabrouk and Spiro (1998).

It should be noted that the increase of B_{1g} distortion has been inferred solely from the ν_{11} of the pc-qms state so that it cannot be assigned to increased population of the hc-hs state obtained from the spectral analysis. The DPR changes of ν_4

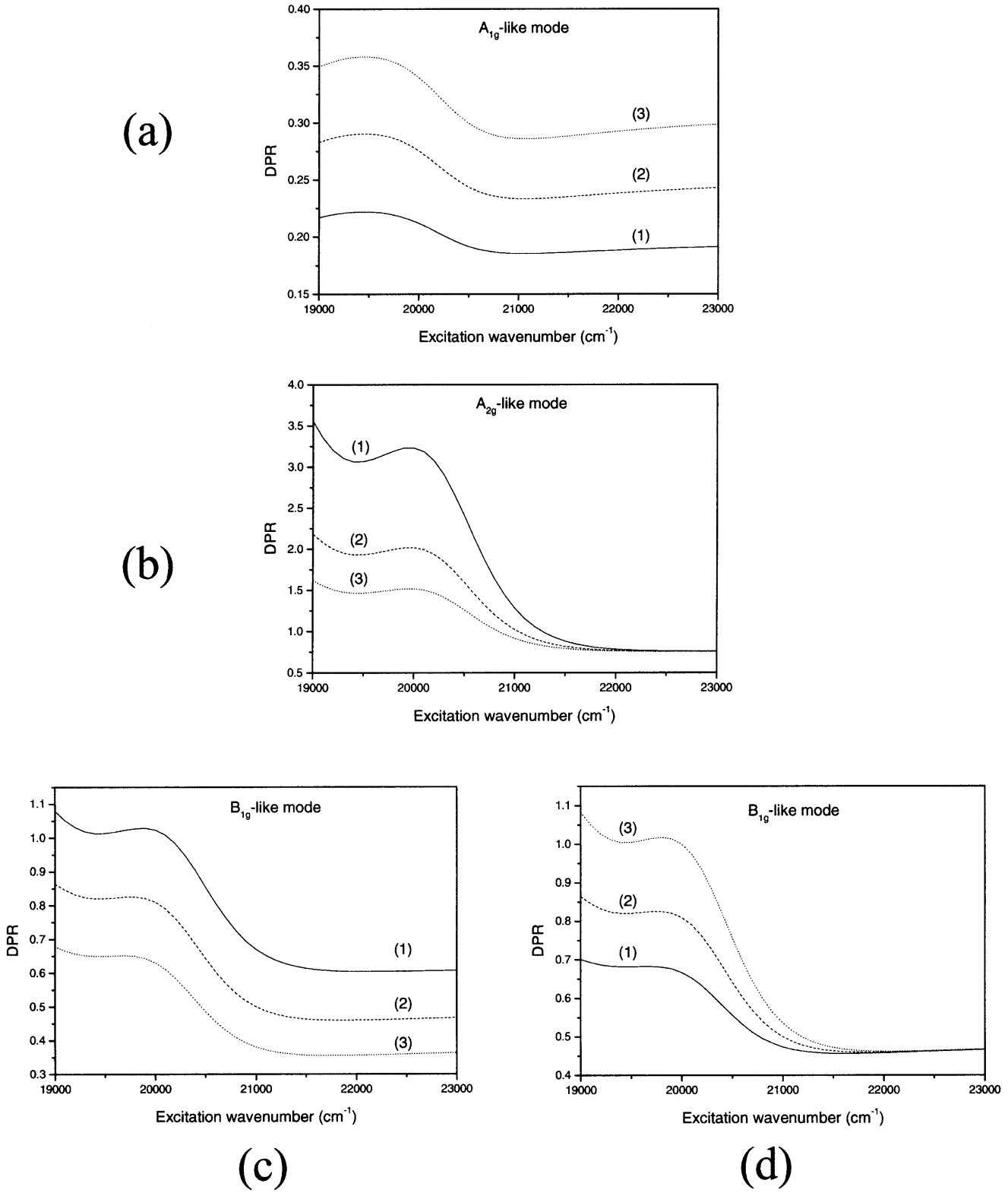

FIGURE 5 Simulation of DPRs for (*a*) A_{1g}like, (*b*) A_{2g}like, and (*c* and *d*) B_{1g}like modes of hemes subject to rhombic distortions. Increase of rhombic distortion is represented by the cases (*1*), (*2*), (*3*) in sequence. For B_{1g}like mode, changes of DPRs upon increasing solely B_{1g} or B_{2g} distortion are illustrated in the cases *c* and *d*, separately.

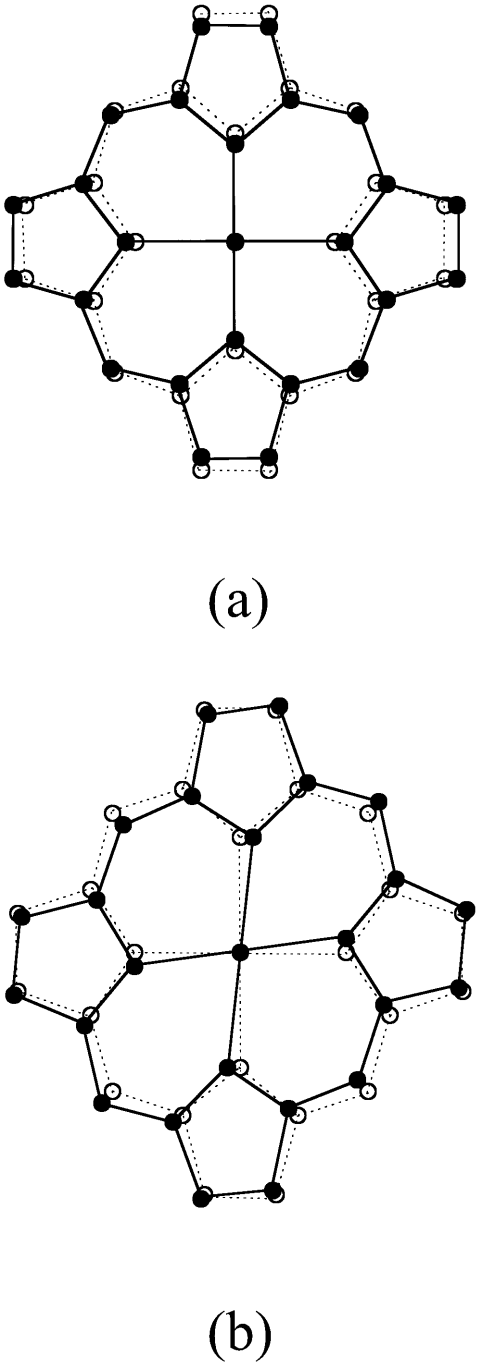

FIGURE 6 A schematic sketch of rhombic (*a*) B_{1g} and (*b*) B_{2g} deformations of the heme macrocycle.

and ν_{21}, however, might also reflect changes caused by the binding of a sixth ligand (i.e., H_2O). Particularly the DPR of ν_4 is known to be very sensitive to interactions between the heme core and axial ligands (Schweitzer-Stenner, 1989). With respect to the sixth ligand, el Naggar et al. (1985) reported a significant and systematic increase of the ν_4 DPR upon oxygen binding to myoglobin.

For HRP-PEG:BHA in water, however, the DPRs of ν_{11} strongly suggest that the interaction between the substrate and the heme gives predominantly rise to B_{2g} distortions. Overall, distortions are between those of HRP-PEG in water and in the investigated aromatic solvents, as expected. Our results are at variance with the deformations obtainable from a normal-coordinate structural decomposition (NSD) analysis of the wild-type HRP:BHA crystal structure, which indicate significantly reduced rhombic B_{1g} and B_{2g} distortions of the heme. On the other hand, however, our data are consistent with spectroscopic studies showing a Q-band splitting of ferrous low spin HRP:BHA-CO spectra, which is absent in the spectra of the corresponding HRP-CO species (Kaposi et al., 2001) and with electron paramagnetic resonance data that indicate that significant rhombicity of the ligand field is maintained upon BHA binding (Indiani et al., 2000). Three explanations can be given for this discrepancy. First, one can interpret them as indicating that the heme structure of HRP in aqueous solution is more distorted than in the crystal. This does not seem unlikely in view of the very flexible and open heme pocket. This notion is not at odds with the finding of Smulevich et al. (1999), who reported nearly identical Raman spectra for HRP:BHA in solution and in a single crystal, since DPR changes reflect variations of the first derivative of the potential surface along the displacement coordinates of low-frequency B_{1g} and B_{2g} modes, whereas frequency changes of a Raman active mode are due to changes of the second derivative of the potential surface with respect to its own normal coordinate. Second, it is in principle possible that the differences between the DPR values of HRPc-PEG and HRPc-PEG:BHA reflect structural differences between the excited electronic states of the respective heme groups rather than between their ground states (Schweitzer-Stenner et al., 2000). Third, one has to take into consideration that the x-ray structure was obtained for genetically engineered HRP without any glycans (Henriksen et al., 1998), whereas all the spectroscopic work was done with HRP in its natural glycolysated form.

Since resonance Raman spectra of Teraoka and Kitagawa (1981) reveal no changes of the 379 cm^{-1} Raman line of the propionate substituent, any interaction of BHA with the respective pyrrole groups are likely to be weak. The crystal structure (Henriksen et al., 1998) exhibits BHA nearly parallel oriented to the heme group and in van der Waals contact with a C_m atom of one of the methine bridges between the two pyrrole groups with methyl and vinyl substituents. This can be expected to give rise to an electronic perturbation of the macrocycle due to $\pi\pi$-interaction. As experimentally and theoretically shown for meso-substituted nitroporphyrins (Schweitzer-Stenner et al., 2001), such a distortion gives rise to B_{2g} and an E_u distortions, in full accordance with our data. This interpretation is further corroborated by the fact that the reaction with BHA has a comparatively strong impact on the DPR of ν_{21}, which is mostly a C_mH bending mode (Li et al., 1990).

In a recent study on native HRPc (Huang et al., 2003), we have invoked group theoretical arguments to show that

particularly a perturbation leading to B_{2g} distortions of the heme can stabilize the intermediate spin state of the iron atom and concomitantly facilitate its interaction with the high spin state by spin orbit coupling (Maltempo, 1974). Maltempo and co-worker (1979) have argued that it should be easier to oxidize the qms then the hs state, which is important for the formation of compound I. Apparently, the protein conformer with a qms iron is still predominant for HRPc-PEG in the investigated organic solvents. For HRP-PEG:BHA, the strong increase of the B_{2g} distortion might be the reason for the very rare hc-qms state inferred from electron paramagnetic resonance data (Indiani et al., 2000). If Maltempo et al. (1979) are right, one expects that the enzyme should exhibit significant enzymatic activity in benzene and toluene. This is in line with findings by Kazadjian et al. (1986). The functional role of the B_{1g} distortion particularly obtained for HRPc-PEG in benzene and toluene is less clear, but it is likely that the respective perturbation also stabilizes the pc-qms state, though somewhat more indirectly than B_{2g} perturbations.

SUMMARY

Taken together, our data provide evidence that the structural integrity of the heme group is maintained when HRP-PEG is dissolved in organic solvents. Some structural changes, however, are induced by benzene and toluene molecules penetrating the heme pocket. This slightly stabilizes the hc-hs state of the heme iron with respect to the dominant pc-qms state observed for native HRP and HRP-PEG in the resting state. In agreement with the hypothesis of Mabrouk and Spiro (1998), our data strongly corroborate the notion that benzene as well as toluene are in close contact with one of the pyrrole groups (most likely that directed toward Phe^{179} and Gln^{176}), which gives rise to an additional B_{1g} type distortion. HRP-BHA in water shows a different mode of interaction in that the contact between BHA and a heme methin carbon gives rise to a B_{2g}-type distortion and to a predominantly hc-hs state. Both distortions are likely to stabilize the qms state of the heme iron, which has been hypothesized to facilitate the metal's oxidation in the compound I formation process. Overall, our studies show that substrate binding (also the aromatic solvent molecules function as substrates) causes changes of the heme deformation, and, of course, it is the thus induced structural state and not that of the native enzyme that determines the heme contribution to the overall enzymatic reactivity.

We thank Prof. John Shelnutt for helpful discussion on the NSD analysis of the heme macrocycle in native HRP and HRP-PEG:BHA, and his kind readiness to help us produce Fig. 6, which illustrates rhombic distortions in NSD analysis. Q.H. thanks Prof. Patricia A. Mabrouk for searching a relevant reference.

The authors acknowledge financial support by grants from the National Institutes of Health (COBRE program P20 RR16439-01 to K.G. and R.S.S.) and the Petroleum Research Funds (PRF 38544-AC4 to R.S.S.)

REFERENCES

Adam, W., M. Lazarus, C. R. Saha-Möller, O. Weichold, U. Hoch, D. Häring, and P. Schreier. 1999. Biotransformations with peroxidases. *Adv. Biochem. Eng. Biotechnol.* 63:74–108.

Akasaka, R., T. Mashino, and M. Hirobe. 1995. Hydroxylation of benzene by horseradish peroxidase and immobilized horseradish peroxidase in an organic solvent. *Bioorg. Med. Chem. Lett.* 5:1861–1864.

Al-Azzam, W., E. A. Pastrana, Y. Ferrer, Q. Huang, R. Schweitzer-Stenner, and K. Griebenow. 2002. Structure of PEG-modified HRP in organic solvents: IR amide I spectral changes upon protein dehydration are largely due to protein structural changes and not to water removal per se. *Biophys. J.* 83:3637–3651.

Asher, S. A., and J. Murtaugh. 1983. Metalloporphyrin gas and condensed-phase resonance Raman studies: the role of vibrational anharmonicities as determinants of Raman frequencies. *J. Am. Chem. Soc.* 105:7244–7251.

DeVito, V. L., M. L. Cai, S. A. Asher, L. A. Kehrens, and K. M. Smith. 1992. UV-resonance Raman evidence for electronically and vibrationally independent protoporphyrin IX vinyl groups. *J. Phys. Chem.* 96:6917–6922.

Dordick, J. S., M. A. Marletta, and A. M. Klibanov. 1986. Peroxidases depolymerize lignin inorganic media but not in water. *Proc. Natl. Acad. Sci. USA.* 83:6255–6257.

Dunford, H. B. 1999. Heme Peroxidases. Wiley-VCH Press, New York.

el Naggar, S., W. Dreybrodt, and R. Schweitzer-Stenner. 1985. Haem-apoprotein interactions detected by resonance Raman scattering in Mb- and Hb-derivatives lacking the saltbridge His^{146} β-$Asp^{94}\beta$. *Eur. Biophys. J.* 12:43–49.

Evangelista-Kirkup, R., M. Crisanti, T. L. Poulos, and T. G. Spiro. 1985. Resonance Raman spectroscopy shows different temperature-dependent coordination equilibria for native horseradish and cytochrome c peroxidase. *FEBS Lett.* 190:221–226.

Faber, K., G. Ottolina, and S. Riva. 1993. Selectivity-enhancement of hydrolase reactions. *Biocatalysis.* 8:91–132.

Feis, A., B. D. Howes, C. Indiani, and G. Smulevich. 1998. Resonance Raman and electronic absorption spectra of horseradish peroxidase isoenzyme A2: evidence for a quantum-mixed spin species. *J. Raman Spectrosc.* 29:933–938.

Ferraro, J. R., and K. Nakamoto. 1994. Introductory Raman Spectroscopy. Academic Press, New York.

Gajhede, M., D. J. Schuller, A. Heriksen, A. T. Smith, and T. L. Poulos. 1997. Crystal structure determination of classical horseradish peroxidase at 2.15 Å resolution. *Nat. Struct. Biol.* 4:1032–1038.

Griebenow, K., Y. Diaz Laureano, A. M. Santos, I. Montañez Clemente, L. Rodriguez, M. Vidal, and G. Barletta. 1999. Improved enzyme activity and enantioselectivity in organic solvents by methyl-β-cyclodextrin. *J. Am. Chem. Soc.* 121:8157–8163.

Griebenow, K., and A. M. Klibanov. 1997. Can conformational changes be responsible for solvent and excipient effects on the catalytic behavior of subtilisin Carlsberg in organic solvents? *Biotechnol. Bioeng.* 53:351–362.

Griebenow, K., M. Vidal, C. Baéz, A. M. Santos, and G. Barletta. 2001. Nativelike enzyme properties are important for optimum activity in neat organic solvents. *J. Am. Chem. Soc.* 123:5380–5381.

Gorman, L. A. S., and J. S. Dordick. 1992. Organic solvents strip water off enzymes. *Biotechnol. Bioeng.* 39:392–397.

Habeeb, A. S. F. A. 1966. Determination of free amino groups in proteins by trinitrobenzenesulfonic acid. *Anal. Biochem.* 14:328–336.

Henriksen, A., D. J. Schuller, K. Meno, K. G. Welinder, A. T. Smith, and M. Gajhede. 1998. Structural interactions between horseradish peroxidase C and the substrate benzhydroxamic acid determined by X-ray crystallography. *Biochemistry.* 37:8054–8060.

Howes, B. D., A. Feis, C. Indiani, M. Marzocchi, and G. Smulevich. 2000. Formation of two types of low-spin heme in horseradish

peroxidase isoenzyme A2 at low temperature. *J. Biol. Inorg. Chem.* 5:227–235.

Howes, B. D., A. Feis, L. Raimondi, C. Indiani, and G. Smulevich. 2001. The critical role of the proximal calcium ion in the structural properties of horseradish peroxidase. *J. Biol. Chem.* 276:40704–40711.

Howes, B. D., J. N. Rodriguez-Lopez, A. T. Smith, and G. Smulevich. 1997. Mutation of distal residues of horseradish peroxidase: influence on substrate binding and cavity properties. *Biochemistry*. 36:1532–1543.

Howes, B. D., C. B. Schiødt, K. G. Welinder, M. P. Marzocchi, J.-G. Ma, J. Zhang, J. A. Shelnutt, and G. Smulevich. 1999. The quantum mixed-spin heme state of barley peroxidase: a paradigm for class III peroxidases. *Biophys. J.* 77:478–492.

Huang, Q., K. Szigeti, J. Fidy, and R. Schweitzer-Stenner. 2003. Structural disorder of native horseradish peroxidase C probed by resonance Raman and low-temperature optical absorption spectroscopy. *J. Phys. Chem. B.* 107:2822–2830.

Indiani, C., A. Feis, B. D. Howes, M. P. Marzocchi, and G. Smulevich. 2000. Benzohydroxamic acid-peroxidase complexes: spectroscopic characterization of a novel heme spin species. *J. Am. Chem. Soc.* 132:7368–7376.

Jentzen, W., J.-G. Ma, and J. A. Shelnutt. 1998. Conservation of the conformation of the porphyrin macrocycle in hemoproteins. *Biophys. J.* 74:753–763.

Jentzen, W., E. Unger, G. Karvounis, J. A. Shelnutt, W. Dreybrodt, and R. Schweitzer-Stenner. 1996. Conformational properties of nickel (II) octaethylporphyrin in solution. 1. Resonance excitation profiles and temperature dependence of structure-sensitive Raman lines. *J. Phys. Chem.* 100:14184–14191.

Kamiya, N., M. Inoue, M. Goto, N. Nakamura, and Y. Naruta. 2000. Catalytic and structural properties of surfactant-horseradish peroxidase complex in organic media. *Biotechnol. Prog.* 16:52–58.

Kaposi, A. D., J. M. Vanderkooi, W. W. Wright, J. Fidy, and S. S. Stavrov. 2001. Influence of static and dynamic disorder on the visible and infrared absorption spectra of carbonmonoxy horseradish peroxidase. *Biophys. J.* 81:3472–3482.

Kazandjian, R. Z., J. S. Dordick, and A. Klibanov. 1986. Enzymatic analyses in organic solvents. *Biotechnol. Bioeng.* 28:417–421.

Klibanov, A. M. 1990. Asymmetric transformations catalyzed by enzymes in organic solvents. *Acc. Chem. Res.* 23:114–120.

Klibanov, A. M. 1997. Why are enzymes less active in organic solvents than in water? *Trends Biotechnol.* 15:97–101.

Lemke, C., W. Dreybrodt, J. A. Shelnutt, J. M. E. Quirke, and R. Schweitzer-Stenner. 1998. Polarized Raman dispersion spectroscopy probes planar and non-planar distortions of Ni (II)-porphyrins with different peripheral substituents. *J. Raman Spectrosc.* 29:945–953.

Li, X.-Y., R. S. Czernuszewicz, J. R. Kincaid, P. Stein, and T. G. Spiro. 1990. Consistent porphyrin force field. 2. Nickel octaethylporphyrin skeletal and substituent mode assignment from 15 N, meso-*d*, and methylene- *d* 16 Raman and infrared isotope shifts. *J. Phys. Chem.* 94: 47–61.

Mabrouk, P. A. 1995. The use of nonaqueous media to probe biochemically significant enzyme intermediates: the generation and stabilization of horseradish peroxidase compound II in neat benzene solution at room temperature. *J. Am. Chem. Soc.* 117:2141–2146.

Mabrouk, P. A. 1997. The use of PEG-enzymes in non-aqueous enzymology. *In* Poly(ethylene Glycol). Chemistry and Biological Applications, Vol. 680. J. M. Harris and S. Zalipsky, editors. American Chemical Society, Washington, D.C. 118–133.

Mabrouk, P. A., and T. G. Spiro. 1998. New insights into horseradish peroxidase function in benzene from resonance Raman spectroscopy. *J. Am. Chem. Soc.* 120:10303–10309.

Maltempo, M. M. 1974. Magnetic state of an unusual bacterial heme. *J. Chem. Phys.* 61:2540–2547.

Maltempo, M. M., P.-I. Ohlsson, K.-G. Paul, and A. Ehrenberg. 1979. Electron paramagnetic resonance analysis of horseradish peroxidase in situ and after purification. *Biochemistry*. 18:2935–2941.

McClain, W. M. 1971. Excited state symmetry assignment through polarized two-photon absorption. Studies of fluid. *J. Chem. Phys.* 55:2789–2796.

Nissum, M., A. Feis, and G. Smulevich. 1998. Characterization of soybean seed coat peroxidase: resonance Raman evidence for a structure-based classification of plant peroxidases. *Biochemistry*. 4:355–364.

Palanappian, V., and J. Terner. 1989. Resonance Raman spectroscopy of horseradish peroxidase derivatives and intermediates with excitation in the near ultraviolet. *J. Biol. Chem.* 264:16046–16053.

Paradkar, V. M., and J. S. Dordick. 1994. Aqueous-like activity of α-chymotrypsin dissolved in nearly anhydrous organic solvents. *J. Am. Chem. Soc.* 116:5009–5010.

Rakshit, G., and T. G. Spiro. 1974. Resonance Raman spectra of horseradish peroxidase: evidence for anomalous heme structure. *Biochemistry*. 13:5317–5323.

Ryu, K., and J. S. Dordick. 1992. How do organic solvents affect peroxidase structure and function? *Biochemistry*. 31:2588–2598.

Schmitke, J. L., C. R. Wescott, and A. M. Klibanov. 1996. The mechanistic dissection of the plunge in enzymatic activity upon transition from water to anhydrous solvents. *J. Am. Chem. Soc.* 118:3360–3365.

Schoffers, E., A. Golebiowski, and C. R. Johnson. 1996. Enantioselective synthesis through enzymatic asymmetrization. *Tetrahedron*. 52:3769–3826.

Schweitzer-Stenner, R. 1989. Allosteric linkage induced distortions of the prosthetic group in haem proteins as derived by the theoretical interpretation of the depolarization ratio in resonance Raman scattering. *Q. Rev. Biophys.* 22:381–479.

Schweitzer-Stenner, R. 2001. Polarized resonance Raman dispersion spectroscopy on metalporphyrins. *J. Porphyrins Phthalocyanines.* 5:198–224.

Schweitzer-Stenner, R., A. Cupane, M. Leone, C. Lemke, J. Schott, and W. Dreybrodt. 2000. Anharmonic protein motions and heme deformations in myoglobin cyanide probed by absorption and resonance Raman spectroscopy. *J. Phys. Chem. B.* 104:4754–4764.

Schweitzer-Stenner, R., W. Dreybrodt, and S. el Naggar. 1984. Investigation of pH-induced symmetry distortions of the prosthetic group in deoxyhaemoglobin by resonance Raman scattering. *Biophys. Struct. Mech.* 10:241–256.

Schweitzer-Stenner, R., W. Jentzen, and W. Dreybrodt. 1993. Anharmonic coupling in nickel(II) octaethylporphyrin investigated by resonance Raman spectroscopy. *In* Fifth International Conference on the Spectroscopy of Biological Molecules. T. Theophanides, J. Anastassopoulo, and N. Fotopoulos, editors. Kluwer Academic Publishers, Dordrecht, the Netherlands. 33–34.

Schweitzer-Stenner, R., C. Lemke, R. Haddard, Y. Qui, J. A. Shelnutt, J. M. E. Quirke, and W. Dreybrodt. 2001. Conformational distortions of metalloporphyrins with electron withdrawing NO_2 substituents at different meso positions. a structural analysis by polarized Raman dispersion spectroscopy and molecular mechanics calculations. *J. Phys. Chem. A.* 105:6680–6694.

Secundo, F., G. Carrea, G. Vecchio, and F. Zambianchi. 1999. Spectroscopic investigation of lipase from Pseudomonas cepacia solubilized in 1,4-dioxane by non-covalent complexation with methoxypoly(ethylene glycol). *Biotechnol. Bioeng.* 64:624–628.

Shelnutt, J. A. 2000. Theoretical and physical characterization. *In* The Porphyrin Handbook, Vol. 7. K. M. Kadish, K. M. Smith, and R. Guilard, editors. Academic Press, New York. 167–220.

Shelnutt, J. A., L. D. Cheung, R. C. C. Chang, N. T. Yu, and R. H. Felton. 1977. Resonance Raman spectra of metalloporphyrins. Effects of Jahn-Teller instability and nuclear distortion on excitation profiles of Stoke fundamentals. *J. Chem. Phys.* 66:3387–3398.

Smulevich, G., A. M. English, A. R. Mantini, and M. P. Marzocchi. 1991. Resonance Raman investigation of ferric iron in horseradish peroxidase and its aromatic donor complexes at room and low temperature. *Biochemistry*. 30:772–779.

Smulevich, G., A. Feis, C. Indiani, M. Becucci, and M. P. Marzocchi. 1999. Peroxidase-benzhydroxamic acid complexes: spectroscopic evidence that

a Fe-H_2O distance of 2.6 Å can correspond to hexa-coordinated high-spin heme. *J. Biol. Inorg. Chem.* 4:39–47.

Smulevich, G., M. Paoli, J. F. Burke, S. A. Sanders, R. N. F. Thorneley, and A. T. Smith. 1994. Characterization of recombinant horseradish peroxidase C and three site-directed mutants, F41V, F41W, and R38K, by resonance Raman spectroscopy. *Biochemistry.* 33:7398–7407.

Spiro, T. G. 1985. Resonance Raman spectroscopy as a probe of heme protein structure and dynamics. *Adv. Prot. Chem.* 37:111–159.

Takahashi, K., H. Nishimura, T. Yoshimoto, Y. Saito, and Y. Inada. 1984. A chemical modification to make horseradish peroxidase soluble and active in benzene. *Biochem. Biophys. Res. Commun.* 121: 261–265.

Teraoka, J., and T. Kitagawa. 1981. Structural implication of the heme-linked ionization of horseradish peroxidase probed by the Fe-histidine stretching Raman line. *J. Biol. Chem.* 256:3969–3977.

Unger, E., U. Bobinger, W. Dreybrodt, and R. Schweitzer-Stenner. 1993. Vibronic coupling in nickel(II) porphine derived from resonant Raman excitation profiles. *J. Phys. Chem.* 97:9956–9978.

Zgierski, M. Z., and M. Pawlikowski. 1982. Depolarization dispersion curves of some Raman fundamentals in ferrocytochrome c and oxyhaemoglobin. *Chem. Phys.* 65:335–367.